

1 **Fossil and Non-fossil Fuel Sources of Organic and Elemental Carbon**
2 **Aerosols in Beijing, Shanghai and Guangzhou: Seasonal Carbon-source**
3 **Variation**

4 Di Liu¹, Matthias Vonwiller², Jun Li^{*1}, Junwen Liu³, Sönke Szidat², Yanlin Zhang⁴, Chongguo
5 Tian⁵, Yinjun Chen⁶, Zhineng Cheng¹, Guangcai Zhong¹, Pingqing Fu⁷, Gan Zhang¹

6 ¹State Key Laboratory of Organic Geochemistry, Guangzhou Institute of Geochemistry,
7 Chinese Academy of Sciences, Guangzhou, 510640, China

8 ²Department of Chemistry and Biochemistry & Oeschger Centre for Climate Change
9 Research, University of Bern, Berne, 3012, Switzerland

10 ³Institute for Environmental and Climate Research, Jinan University, Guangzhou, 511443,
11 China

12 ⁴Yale-NUIST Center on Atmospheric Environment, International Joint Laboratory on Climate
13 and Environment Change (ILCEC), Nanjing University of Information Science and Technology,
14 Nanjing 210044, China

15 ⁵Key Laboratory of Coastal Environmental Processes and Ecological Remediation, Yantai
16 Institute of Coastal Zone Research, Chinese Academy of Sciences, Yantai 264003, China

17 ⁶State Key Laboratory of Pollution Control and Resources Reuse, Key Laboratory of
18 Cities' Mitigation and Adaptation to Climate Change, College of Environmental Science
19 and Engineering, Tongji University, Shanghai 200092, China

20 ⁷ Institute of Surface-Earth System Science, Tianjin University, Tianjin 300072, China

21 *To whom correspondence may be addressed:

22 Dr. Jun Li; Email: junli@gig.ac.cn; Tel.: +86-20-85291508; Fax: +86-20-85290706

23

24 **Abstract**

25 Fossil fuel (FF) combustion and non-fossil fuel (NF) emissions (such as biomass
26 burning) are the two most important contributors to the high air pollution in China.
27 Within the large territorial area of China, these two emission sources may exert
28 different influences on the carbonaceous particles sampled in megacities among
29 regions and seasons. Here, the radiocarbon isotopic signals in Beijing, Shanghai and
30 Guangzhou, China from 2013 to 2014 are reported. Generally, a greater contribution
31 of NF (>55%) sources was found in all cities during autumn. However, source
32 seasonality differed among cities during the other seasons. During winter, FF
33 contributed to the majority of pollution in Beijing (64%), NF contributed to the
34 majority in Guangzhou (63%), and FF contributed slightly more than NF in Shanghai
35 (54%). During spring and summer, Beijing and Guangzhou showed similar patterns,
36 with higher contributions from FF (55% and 63%, respectively) than NF. FF made the
37 greatest contribution (71%) in Shanghai during summer. Secondary organic carbon
38 originated mainly from biomass burning and vehicle emissions, except in Beijing
39 during winter, when the major source was residual coal combustion.

40 **Introduction**

41 Large-scale pollution of fine particles (aerodynamic diameter $\leq 2.5 \mu\text{m}$; $\text{PM}_{2.5}$)
42 occurs frequently, impacting air quality in the megacities of China due to massive and
43 intensive pollutant emissions combined with unfavorable meteorological conditions.
44 Among aerosol pollutants, carbonaceous aerosols, which can constitute 20–50% of
45 aerosols in the urban atmosphere,(Cao et al., 2007) are of great concern due to their

46 adverse impacts on air quality, visibility, human health and climate.(Highwood and
47 Kinnersley, 2006;Mauderly and Chow, 2008;Pratsinis et al., 1984) Carbonaceous
48 materials are operationally classified as strongly refractory, highly polymerized
49 carbon (elemental carbon, EC) and black carbon (BC) or weakly refractory, light
50 polycyclic or polyacidic hydrocarbon (organic carbon, OC).(Castro et al., 1999;Pöschl,
51 2005) EC originates exclusively from primary sources and is emitted during
52 incomplete combustion of fossil fuels (FFs; i.e., coal and petroleum) and biomass
53 burning (BB; i.e., heating and wood fires). OC is a complex mixture of primary
54 (directly emitted) OC (POC) and secondary OC (SOC) particles formed in situ in the
55 atmosphere via oxidation of gas-phase precursors. Using a recently developed
56 method, source apportionment can be determined by measuring the radiocarbon
57 (^{14}C) content of OC and EC separately, which enables unambiguous differentiation
58 between FF and non-FF (NF) sources.(Liu et al., 2013;Zong et al., 2016;Liu et al.,
59 2016;Liu et al., 2014;Liu et al., 2017c;Zhang et al., 2015a) This differentiation is
60 possible because ^{14}C is completely decayed in FF sources (i.e., diesel exhaust,
61 gasoline exhaust and coal combustion), whereas NF sources (i.e., BB, cooking and
62 biogenic emissions) exhibit contemporary ^{14}C levels.(Szidat et al., 2009) Even more
63 precise ^{14}C -based source apportionment can be obtained by dividing OC into
64 water-soluble OC and water-insoluble OC.(Liu et al., 2016)

65 Beijing, Shanghai and Guangzhou are representative megacities located in different
66 climatic regions (the Beijing–Tianjin–Hebei region, Yangtze River Delta region and
67 Pearl River Delta region, respectively) that suffer from severe air pollution due to

68 rapid expansion of industry and transportation, sharply increasing the population and
69 thus the demand for FFs.(Feng et al., 2015;Wei et al., 2017;Ding et al., 2017;Zhang et
70 al., 2015a;Ling et al., 2011) Although source apportionment of carbonaceous
71 aerosols has been conducted in some cities,(Wei et al., 2017;Liu et al., 2014;Liu et al.,
72 2017c;Elser et al., 2016;Liu et al., 2018) the results are segmented and generally
73 pertain to haze events during winter. In our previous research, several independent
74 case studies were conducted in Guangzhou. For example, during winter (Nov. 29,
75 2012 to Jan. 19, 2013), higher contributions of FF sources to EC (80–90%) were
76 observed for haze samples that were substantially impacted by local emissions, and
77 lower contributions of FF to EC (60–70%) were found for haze particles impacted by
78 regional transport.(Liu et al., 2014) During Spring (Mar. 15 to Apr. 15 2013), NF
79 sources majorly contributed to total carbonaceous aerosols ($46 \pm 5\%$).(Liu et al., 2016)
80 During summer (June 25, 2013 to July 15, 2013), 87% of EC and 53% of OC in $PM_{2.5}$
81 were derived from FF sources on a typical summer day, but these values dropped
82 significantly with invasion of NF-enriched air masses from rural and suburban
83 areas.(Liu et al., 2018) During autumn (Oct. 15 2013 to Nov. 15 2013), NF was the
84 predominant source of total carbon (TC; average = $65 \pm 7\%$).(Liu et al., 2017a) In this
85 study, a $PM_{2.5}$ sampling campaign was conducted simultaneously in three cities over
86 1 year, and two samples with relatively high and low $PM_{2.5}$ concentrations during
87 each season in the three cities were selected for ^{14}C analysis. ^{14}C data of ambient
88 aerosols from Beijing, Shanghai and Guangzhou are presented for these two
89 sub-fractions in terms of TC, OC and EC. Furthermore, OC was divided into

90 water-insoluble OC and water-soluble OC. A comparison of the sources and seasonal
91 variation of carbonaceous aerosols among the three cities was conducted. The
92 results can help identify the carbon sources of aerosols in China and support
93 policymakers in developing appropriate air-quality management initiatives for
94 particulate matter pollution.

95 **2. Methods and experiments**

96 **2.1 Aerosol sampling**

97 PM_{2.5} samples were collected in Beijing, Shanghai and Guangzhou during the four
98 seasons. Detailed descriptions of the sampling sites, sampling methods and protocols
99 have been described previously.(Liu et al., 2017a) Briefly, four sampling periods were
100 selected to represent the four seasons: autumn (October 16 to November 15, 2013),
101 winter (December 20, 2013 to January 20, 2014), spring (March 20 to April 20, 2014),
102 and summer (June 20 to July 20, 2014). During each season, 24-h integrated PM_{2.5}
103 samples were collected on pre-heated (450 °C for 5 h) quartz fiber filters (8 × 10 in;
104 Whatman, UK or PALL, USA) using a high-volume sampler (Shanghai Xintuo) at a flow
105 rate of 0.3 m³ min⁻¹. In this study, we collected 110, 110 and 106 samples from
106 Beijing, Shanghai and Guangzhou, respectively. At each sampling site and season,
107 one field blank sample was collected and analyzed. All samples were stored at -20 °C
108 until analysis.

109 **2.2. Thermal–optical carbon analysis**

110 Portions of the filter samples (1.5 cm²) were cut for analysis of the OC and EC
111 contents (OC/EC) using a thermal–optical carbon analyzer (Sunset Laboratory Inc.,

112 Forest Grove, OR, USA) following a modified National Institute of Occupational Safety
113 and Health (NIOSH) thermal–optical transmission protocol. NIOSH thermal–optical
114 transmission and the Interagency Monitoring of Protected Visual Environments
115 (IMPROVE) thermal–optical reflectance are two common thermal–optical methods.
116 Due to differences in charring correction and the temperature program, the
117 NIOSH-defined EC concentration was slightly lower than that defined by IMPROVE,
118 although the TC concentrations measured by the two methods were
119 comparable.(Cheng et al., 2011) Replicate samples and a filter blank were conducted
120 to determine the analytical precision and identify background contamination.
121 Analysis of replicate samples (n = 64) provided good analytical precision, with relative
122 deviations of 4.5%, 8.6% and 4.5% for OC, EC and TC, respectively. The average field
123 blank concentration of OC was $1.47 \pm 0.17 \mu\text{g cm}^{-2}$ (1σ , n = 12), and that of EC was
124 undetectable. The lowest OC value observed on a filter was $\sim 10 \mu\text{g cm}^{-2}$ before
125 subtraction of the blank value. The reported OC concentrations were adjusted by
126 subtraction of the values of the filter blanks. Field blanks were not analyzed for OC
127 and EC ^{14}C .

128 **2.3. ^{14}C analysis of the carbonaceous fractions**

129 ^{14}C was measured in carbonaceous aerosols to distinguish FF and NF sources
130 quantitatively. Two samples with relatively high and low $\text{PM}_{2.5}$ concentrations
131 collected in each season and city were selected for ^{14}C analysis, although only one
132 sample was analyzed during summer in Shanghai (23 samples total). The 3-day air
133 mass back trajectories for all selected samples are shown in Fig. 1. The detailed

134 method of ^{14}C measurement in various carbonaceous aerosols (i.e., TC, EC and
135 water-soluble OC (WSOC)) has been described elsewhere.(Zhang et al., 2012;Zhang
136 et al., 2015a) Recently, ^{14}C measurements in aerosols collected in China were
137 analyzed following this protocol.(Huang et al., 2014) Briefly, the ^{14}C content of TC was
138 analyzed through coupling of an elemental analyzer with a MIni CARbon Dating
139 System (MICADAS) at the University of Bern, Switzerland.(Szidat et al., 2014) ^{14}C
140 analysis of EC and water-insoluble OC (WIOC) were carried out through online
141 coupling of the MICADAS with a Sunset Lab OC/EC analyzer, and the CO_2 resulting
142 from EC or WIOC was separated during either the EC or OC step of the Swiss_4S
143 protocol.(Agrios et al., 2015;Zhang et al., 2012) The ^{14}C analysis results were
144 expressed as fractions of modern carbon (f_M). The f_M values for OC were not
145 measured directly but were deduced through subtraction of TC and EC based on
146 mass balancing. Similarly, the f_M values of WSOC were further calculated via mass
147 balancing through subtraction of OC and WIOC. The average uncertainties of f_M
148 values for OC, EC, TC and WSOC were <10%, including uncertainties from ^{14}C
149 measurements, blank correction and mass-balance calculations.

150 **3. Results and discussion**

151 **3.1 Seasonal variation and concentrations of $\text{PM}_{2.5}$, OC and EC**

152 Fig. 2 shows box-and-whisker plots for the concentrations of $\text{PM}_{2.5}$, OC and EC and
153 EC/OC ratios during the sampling campaign at all three sites. The average $\text{PM}_{2.5}$ mass
154 concentrations in Beijing, Shanghai and Guangzhou were $182 \pm 78.3 \mu\text{g m}^{-3}$, $88.6 \pm$
155 $49.4 \mu\text{g m}^{-3}$ and $80.4 \pm 30.7 \mu\text{g m}^{-3}$, respectively. Despite large variations in the $\text{PM}_{2.5}$

156 levels observed at all sites, concentrations were generally higher in Beijing than in
157 Shanghai or Guangzhou. This result indicates poorer air quality in northern China,
158 which is consistent with previous studies.(Hu et al., 2014)

159 On average, the highest concentrations of OC and EC in PM_{2.5} were observed in
160 Beijing (21.1 ± 13.9 µg m⁻³ and 2.8 ± 2.2 µg m⁻³), followed by Guangzhou (17.3 ± 9.6
161 µg m⁻³ and 2.9 ± 1.3 µg m⁻³) and Shanghai (9.0 ± 7.6 µg m⁻³ and 1.6 ± 1.5 µg m⁻³). The
162 percentages of TC matter (TCM = 1.6 × OC + EC) to total fine particle mass were 20 ±
163 6%, 17 ± 6% and 36 ± 8% in Beijing, Shanghai and Guangzhou, respectively, indicating
164 the importance of carbonaceous aerosols in air quality, especially in Guangzhou,
165 South China. However, no significant correlations were found between the ratio of
166 TCM/PM_{2.5} and PM_{2.5} concentration in Beijing and Shanghai, indicating that
167 carbonaceous aerosols are the major component of PM_{2.5} but did not play a
168 predominant role when PM_{2.5} concentrations were higher. On the other hand, in
169 Guangzhou, the ratio of TCM/PM_{2.5} was positively correlated with the PM_{2.5}
170 concentration (R² = 0.27, p<0.05). This finding shows that the relative contributions
171 of carbonaceous aerosols to total fine particles increased with increasing PM_{2.5}
172 concentrations in Guangzhou, implying that the role of carbonaceous aerosols in
173 PM_{2.5} is greater in South China than in other parts of China. The average
174 concentrations of OC and EC in Beijing, Shanghai and Guangzhou in this study were
175 similar to those reported in the same respective cities in 2013 (OC: 38.6 µg m⁻³; EC:
176 5.83 µg m⁻³ in Beijing; 10.9 µg m⁻³ and 3.03 µg m⁻³ in Shanghai; 14.4 µg m⁻³ and 3.87
177 µg m⁻³ in Guangzhou)(Zhang et al., 2016) but were significantly higher than those in

178 European urban cities such as Athens, Greece ($2.1 \pm 1.3 \mu\text{g m}^{-3}$ and $0.54 \pm 0.39 \mu\text{g}$
179 m^{-3})(Paraskevopoulou et al., 2014) and Elche, Spain ($5.6 \pm 2.8 \mu\text{g m}^{-3}$ and $1.5 \pm 1.2 \mu\text{g}$
180 m^{-3})(Perrone et al., 2011) and in other Asian urban cities such as Seoul, Korea ($10.2 \pm$
181 $5.5 \mu\text{g m}^{-3}$ and $4.1 \pm 2.6 \mu\text{g m}^{-3}$)(Kim et al., 2007) and Yokohama, Japan ($3.75 \pm 1.5 \mu\text{g}$
182 m^{-3} and $1.94 \pm 1.2 \mu\text{g m}^{-3}$).(Khan et al., 2010)

183 The seasonal variations of $\text{PM}_{2.5}$, OC and EC were characterized by mass
184 concentrations that were higher during winter and lower during summer (Fig. 2). The
185 high winter concentrations can be attributed mainly to a combination of complex
186 effects, such as increasing emissions from local and regional coal and biomass or
187 biofuel combustion and the associated secondary formation processes, as well as
188 unfavorable metrological conditions for pollution dispersal.(Huang et al., 2014)
189 Conversely, the low mass concentrations during summer are likely due to a sharp
190 decrease in anthropogenic source emissions (i.e., heating-related coal and biofuel
191 burning), relatively high wet-scavenging effects and a high mixing layer. (Zhang et al.,
192 2017)

193 Generally, the relationship between OC and EC can give some indication of the origin
194 of carbonaceous particles. A strong relationship between OC and EC might indicate
195 that the carbonaceous particles are derived from the same emission source. Lower
196 OC/EC ratios (1.0–4.2) imply sources from diesel- and gasoline-powered vehicular
197 exhaust,(Schauer et al., 2002, 1999) whereas aerosols with higher OC/EC ratios
198 might originate from coal combustion,(Zhi et al., 2008) wood combustion
199 (16.8–40.0),(Schauer et al., 2001) forest fires (14.5), BB (7.7),(Zhang et al., 2007) or

200 formation of SOC.(Chow et al., 1993) The correlations between OC and EC ($R^2 = 0.56$
201 and 0.80, respectively) were higher in Beijing and Shanghai than in Guangzhou ($R^2 =$
202 0.26). Moreover, the correlations of OC with EC and the OC/EC ratio during different
203 seasons in Beijing and Shanghai were generally consistent. This consistency implies
204 that the sources of the carbonaceous aerosols in Beijing did not change drastically,
205 and that these aerosols were derived from various mixtures. This characteristic was
206 also observed in Shanghai, although the sources of the carbonaceous aerosols
207 differed between the two cities. In Guangzhou, higher correlations between OC and
208 EC during autumn ($R^2 = 0.71$) and winter ($R^2 = 0.50$) were found, with a lower
209 correlation during spring ($R^2 = 0.38$) and no significant correlation during summer.
210 The average OC/EC ratios were significantly ($p < 0.01$) higher during autumn (8.6)
211 and winter (9.6) than spring (4.9) and summer (3.7) (Fig. 2). This finding suggests that
212 the major sources of carbonaceous aerosols differed markedly during different
213 seasons in Guangzhou. The south China region is strongly influenced by
214 anthropogenic emissions from the upwind Asian continent. Analysis of 3-day back
215 trajectories showed that seasonal variations of carbonaceous aerosols were
216 consistent with alteration of the winter and summer monsoons (Fig. 1b); therefore,
217 the major sources of carbonaceous aerosols originated from inland China during
218 autumn and winter but from the Pearl River Delta during spring and summer. This
219 difference in sources likely contributes to the significant seasonal differences in
220 carbonaceous aerosols, which may be elucidated by the ^{14}C results.

221 **3.2 ^{14}C results: f_M and seasonal variation**

222 The concentrations of different carbon species and their ratios in selected samples
223 from three cities are listed in Table 1, and the proportion (%) of FF sources in various
224 carbon fractions of the corresponding samples are shown in Table 2. Overall, FF
225 sources accounted for slightly greater contributions to TC in the three cities annually
226 (average: $53 \pm 10\%$; range: 31–71%) than those of NF sources (average: $47 \pm 10\%$;
227 range: 29–69%), and the values in all three cities were similar. For example, the FF:NF
228 ratios in Beijing, Shanghai and Guangzhou were 54:46, 53:47 and 52:48, respectively.
229 Despite the wide range of EC concentrations (Table 1), the ratios of fossil EC (EC_f) to
230 total EC in Beijing, Shanghai and Guangzhou were comparable, with averages of $73 \pm$
231 6% , $72 \pm 6\%$ and $74 \pm 14\%$, respectively, suggesting that FF combustion is the
232 dominant contributor to EC. The high annual contribution of FFs to EC in the three
233 cities was consistent with previously reports based on a similar ^{14}C -based approach
234 for analyzing EC in cities in China, including Beijing (79% and 82%),(Zhang et al.,
235 2015b;Zhang et al., 2015a) Xi'an ($78 \pm 3\%$),(Zhang et al., 2015a) Shanghai
236 (79%)(Zhang et al., 2015a) and Guangzhou (80–90%),(Liu et al., 2014) as well as
237 previous studies conducted in other cities around the world.(Andersson et al.,
238 2015;Bernardoni et al., 2013;Liu et al., 2013) The average contributions of fossil OC
239 (OC_f) to OC were $50 \pm 10\%$, $49 \pm 9\%$ and $45 \pm 10\%$ in Beijing, Shanghai, and
240 Guangzhou, respectively, which were lower than the corresponding EC_f contributions
241 in all samples. The high proportion of OC_{nf} (32–72%) indicated that primary emissions
242 and secondary formation from NF sources (i.e., BB and biogenic emissions) are
243 important contributors to OC in densely populated urbanized areas of China.

244 The relative contributions of FF and NF sources to EC, WIOC and WSOC in each of the
245 four seasons are plotted in Fig. 3. Distinct seasonal patterns were found in the three
246 cities. Generally, relatively high contributions of NF sources (54–59%) to TC were
247 found during autumn (late October to early November). Particulate EC was
248 predominantly derived from the combustion of FFs such as coal, gasoline and diesel
249 and burning of vegetation and wood (NF sources). In this study, the proportion of EC
250 derived primarily from BB was also higher during autumn (>30%) than during the
251 other seasons. Three-day back trajectory analysis revealed air masses that arrived
252 from inland central China (Fig. 1). Burning of agricultural waste has been suggested
253 to have a strong impact on air quality during this season in Beijing.(Zhang et al., 2017)
254 That result is consistent with our previous study, which indicated that NF emissions
255 were predominant in carbonaceous aerosols in Chinese cities during this season.(Liu
256 et al., 2017a)

257 During winter, the carbon source compositions of the cities differed. The percentage
258 of FF-derived sources was increased significantly in Beijing. $WIOC_f$ and EC_f were
259 generally considered to be primary emissions from coal combustion and vehicle
260 exhaust. Generally, the $WIOC_f/EC_f$ ratios of coal combustion were higher than those
261 of vehicle emissions. The highest $WIOC_f/EC_f$ ratio in this study, 2.39, was obtained in
262 Beijing during winter; this suggests that the increase in the FF-derived contribution
263 was associated with increasing emissions from coal combustion for heating purposes
264 during the cold season in North China (Fig. 1a), which was confirmed by the aerosol
265 mass spectrometer measurements obtained during the same season.(Elser et al.,

266 2016) Based on another study, this FF source enhancement might be attributed to
267 residential coal combustion.(Liu et al., 2017c) In Shanghai, the contribution of fossil
268 carbon increased approximately 11%. The $WIOC_f/EC_f$ ratio of 1.3 indicated that the
269 FF-derived carbon source was a mixture of coal combustion and vehicle emissions. In
270 Guangzhou, the contribution of NF sources was the highest (69%), and the EC_{BB}/EC
271 ratio reached 0.39 and 0.48 in winter samples. As shown in Fig. 1, air masses arrived
272 from the north of Guangdong, Hunan and Guizhou Provinces, where a large amount
273 of biomass, including agricultural waste and hard wood, was burned for cooking and
274 domestic heating during the cold, dry winter. This carbon source characterization
275 matches that reported for regional-scale haze events in a previous study.(Liu et al.,
276 2014)

277 In Beijing and Guangzhou, the source compositions were generally consistent during
278 spring and summer, but the average contribution of NF sources in Beijing ($45 \pm 4\%$)
279 was higher than that in Guangzhou ($37 \pm 3\%$). The results of 3-day back trajectory
280 analysis indicated that natural and biogenic emissions from upwind rural and
281 mountainous areas strongly impacted the air quality in Beijing, whereas the major
282 carbon sources in Guangzhou were from vehicle and industrial emissions in the Pearl
283 River Delta region. In Shanghai, the carbon source composition during spring was
284 most similar to that during winter, but a dramatic increase in FF-derived carbon was
285 observed during summer. The limited sample numbers during summer in Shanghai
286 might have led to biased results. On the other hand, a recent study indicated that the
287 greatest ratio of primary ship-emitted particles to total particles in the Shanghai

288 urban region could reach 50% during ship plume cases, which usually occur during
289 spring and summer. (Liu et al., 2017b) The corresponding back trajectory showed
290 that the air mass came from the East China Sea and passed over the eastern coast of
291 China. In addition to pollutants from industrial and vehicle emissions, the
292 contribution of emissions from fishing boats and large ships near the air-sampling
293 site in Shanghai cannot be ignored.

294 Above all, this study demonstrated that the main sources of carbonaceous aerosols
295 in cities varies greatly among seasons. In Beijing, the seasonal variation was similar to
296 variations in submicrometer organic aerosols measured from 2013 to 2014. (Zhang et
297 al., 2017) Table 3 lists the ^{14}C results from $\text{PM}_{2.5}$ in three cities during 2012–2014
298 published in previous studies. Compared with previous studies, the seasonal
299 variations of carbon sources in the three cities were highly consistent with previous
300 observations conducted in different seasons.(Liu et al., 2014;Liu et al., 2017c;Liu et al.,
301 2016;Liu et al., 2018) The carbon sources of high- $\text{PM}_{2.5}$ samples and low- $\text{PM}_{2.5}$
302 samples from each season were nearly consistent in this study (Fig. 3). Due to the
303 limited data, these results might not reflect the true source variation over a 1-year
304 period. For example, carbon source dynamics of carbonaceous aerosols during haze
305 formation in Guangzhou indicated that there are significant differences in the carbon
306 sources of high- $\text{PM}_{2.5}$ samples and low- $\text{PM}_{2.5}$ samples during spring and summer.(Liu
307 et al., 2018;Liu et al., 2016) In addition, carbon sources of the high- $\text{PM}_{2.5}$ samples in
308 Guangzhou winter also differ from each other.(Liu et al., 2014) In those previous
309 studies, variation of the carbon source of atmospheric aerosols is often affected by

310 changes in meteorological conditions, such as wind direction and speed. In this study,
311 the air masses of the high- and low-PM_{2.5} samples during each season and at each
312 site originated from approximately the same direction (Fig. 1), following the average
313 wind direction of this season. Thus, the results of this study may reflect regional
314 pollution characteristic during different seasons in each city.

315 **3.3 Possible sources of secondary organic aerosols**

316 Based on water solubility, OC was separated into WSOC and WIOC. EC and WIOC
317 were generally considered primary emissions, whereas WSOC was a proxy for
318 secondary OC (SOC) and BB OC.(Zhang et al., 2017) Previous studies have indicated
319 that SOC is the predominant component of WSOC in cities.(Huang et al., 2014;Liu et
320 al., 2016) In this study, WSOC accounted for $47 \pm 7\%$, $32 \pm 7\%$ and $43 \pm 12\%$ of TC in
321 Beijing, Shanghai and Guangzhou, respectively, and was significantly positively
322 correlated with PM_{2.5} concentrations, showing the importance of WSOC in megacities.
323 Moreover, the WSOC/PM_{2.5} ratio was significantly positive correlated with the PM_{2.5}
324 concentration in Beijing ($R^2 = 0.67$, $p < 0.01$) and Guangzhou ($R^2 = 0.31$, $p < 0.05$), but
325 no significant correlation was found in Shanghai. This finding suggests that SOC plays
326 an important role in high-PM_{2.5} events in Beijing and Guangzhou.

327 The potential major sources of WSOC may be revealed by plotting our data. As shown
328 in Fig. 4A, the percentage of non-fossil WSOC to TC was positively correlated with the
329 ratio of EC_{BB}/EC. EC is exclusively of primary origin and is emitted from incomplete
330 combustion of FFs and BB. This correlation indicates that the increase in non-fossil
331 WSOC is likely due to enhanced BB. On one hand, a large fraction of the POC from BB

332 is water soluble; on the other hand, increased emission of volatile organic
333 compounds during BB could lead to an increase in NF secondary organic aerosols.
334 This suggests that BB emissions have an important impact on non-fossil SOC in China.
335 Recently, evidence from a secondary organic aerosol tracer indicated that a large
336 nationwide increase in secondary organic aerosols during the cold season was highly
337 associated with an increase in BB emissions(Ding et al., 2017). In principle, fresh POC
338 emitted from FF combustion is water insoluble. A previous study evaluated the
339 differences in WSOC levels at sites with no direct influence from vehicle exhaust
340 emissions and concluded that very little primary WSOC is emitted directly from
341 vehicles.(Weber et al., 2007) Regarding another type of FF, only ~1% of coal-sourced
342 fresh OC is water soluble.(Park et al., 2012) Thus, POC derived from FF combustion
343 can reasonably be considered water insoluble, and fossil WSOC is used to estimate
344 the levels of FF-derived SOC.(Weber et al., 2007) The fossil WSOC/TC ratio versus the
345 $WIOC_f/EC_f$ ratio is plotted in Fig. 4B. The primary sources of $WIOC_f$ and EC_f were coal
346 combustion and emissions from internal combustion engines fueled by petroleum.
347 Generally, the $WIOC_f/EC_f$ ratio from coal combustion was higher than that from
348 vehicle emissions.(Liu et al., 2013) As shown in Fig. 4B, the proportion of $WSOC_f$
349 decreased with increasing $WIOC_f/EC_f$ ratios in Shanghai and Guangzhou, indicating
350 that fossil SOC did not originate mainly from coal combustion sources, but rather
351 from vehicle and ship emissions or volatile organic compounds (VOCs) released from
352 industrial sources. However, the trend differed in Beijing. Excluding winter samples,
353 the pattern in Beijing was similar to those in Shanghai and Guangzhou, but the trend

354 shifted to the opposite of those in Shanghai and Guangzhou when the winter
355 samples were included. These results suggest that the fossil SOC in Beijing is sourced
356 mainly from residential coal combustion during winter and from vehicle exhaust or
357 industrial emissions during other seasons.

358 **4. Conclusion**

359 Carbonaceous aerosols accounted for $20 \pm 6\%$, $17 \pm 6\%$ and $36 \pm 8\%$ of the mass of
360 $PM_{2.5}$ in Beijing, Shanghai and Guangzhou, respectively. The seasonal variation of
361 $PM_{2.5}$, OC and EC were characterized by mass concentrations that were higher during
362 winter and lower during summer. Based on ^{14}C measurements, the yearly average
363 contributions of FF and NF to TC were almost equal, with FF:NF ratios of 54:46, 53:47
364 and 52:48 in Beijing, Shanghai and Guangzhou, respectively. FF combustion is the
365 dominant contributor to EC (>72%), whereas NF contributes to a slightly higher
366 proportion of OC (50–55%) than does FF at the three sites. Generally, a greater
367 contribution of NF (>55%) sources was found during autumn in all cities. The source
368 seasonality differed among the three cities during the other seasons. During winter,
369 FF contributed more in Beijing (64%), NF in Guangzhou (63%) and FF in Shanghai
370 (54%). During spring and summer, Beijing and Guangzhou had similar source
371 compositions, with higher contributions from FF (55% and 63%, respectively) than NF.
372 However, FF had the highest contribution (71%) in Shanghai during summer. SOC
373 originated mainly from BB and FF oil emissions, except during winter in Beijing, when
374 the major source was residual coal combustion.

375

376

377

378

379 Agrios, K., Salazar, G., Zhang, Y.-L., Uglietti, C., Battaglia, M., Luginbühl, M., Ciobanu, V. G.,

380 Vonwiller, M., and Szidat, S.: Online coupling of pure O₂ thermo-optical methods—14 C AMS

381 for source apportionment of carbonaceous aerosols, *Nuclear Instruments and Methods in*

382 *Physics Research Section B: Beam Interactions with Materials and Atoms*, 361, 288-293, 2015.

383 Andersson, A., Deng, J., Du, K., Yan, C., Zheng, M., Sköld, M., and Gustafsson, O.:

384 Regionally-varying combustion sources of the January 2013 severe haze events over eastern

385 China, *Environmental science & technology*, 2015.

386 Bernardoni, V., Calzolari, G., Chiari, M., Fedi, M., Lucarelli, F., Nava, S., Piazzalunga, A., Riccobono,

387 F., Taccetti, F., and Valli, G.: Radiocarbon analysis on organic and elemental carbon in aerosol

388 samples and source apportionment at an urban site in Northern Italy, *Journal of Aerosol*

389 *Science*, 56, 88-99, 2013.

390 Cao, J. J., Lee, S. C., Chow, J. C., Watson, J. G., Ho, K. F., Zhang, R. J., Jin, Z. D., Shen, Z. X., Chen,

391 G. C., Kang, Y. M., Zou, S. C., Zhang, L. Z., Qi, S. H., Dai, M. H., Cheng, Y., and Hu, K.: Spatial and

392 seasonal distributions of carbonaceous aerosols over China, *Journal of Geophysical Research:*

393 *Atmospheres*, 112, n/a-n/a, 10.1029/2006JD008205, 2007.

394 Castro, L. M., Pio, C. A., Harrison, R. M., and Smith, D. J. T.: Carbonaceous aerosol in urban and

395 rural European atmospheres: estimation of secondary organic carbon concentrations,

396 *Atmospheric Environment*, 33, 2771-2781, [http://dx.doi.org/10.1016/S1352-2310\(98\)00331-8](http://dx.doi.org/10.1016/S1352-2310(98)00331-8),

397 1999.

398 Cheng, Y. A., Zhen, M., He, K. B., Chen, Y. J., Yan, B., Russell, A. G., Shi, W. Y., Jiao, Z., Sheng, G.

399 Y., Fu, J. M., and Edgerton, E. S.: Comparison of two thermal-optical methods for the

400 determination of organic carbon and elemental carbon: Results from the southeastern United
401 States, *Atmospheric Environment*, 45, 1913-1918, 10.1016/j.atmosenv.2011.01.036, 2011.

402 Chow, J. C., Watson, J. G., Pritchett, L. C., Pierson, W. R., Frazier, C. A., and Purcell, R. G.: The Dri
403 Thermal Optical Reflectance Carbon Analysis System - Description, Evaluation and Applications
404 in United-States Air-Quality Studies, *Atmospheric Environment Part a-General Topics*, 27,
405 1185-1201, 1993.

406 Ding, X., Zhang, Y. Q., He, Q. F., Yu, Q. Q., Wang, J. Q., Shen, R. Q., Song, W., Wang, Y. S., and
407 Wang, X. M.: Significant Increase of Aromatics-Derived Secondary Organic Aerosol during Fall
408 to Winter in China, *Environmental Science & Technology*, 51, 7432-7441,
409 10.1021/acs.est.6b06408, 2017.

410 Elser, M., Huang, R. J., Wolf, R., Slowik, J. G., Wang, Q. Y., Canonaco, F., Li, G. H., Bozzetti, C.,
411 Daellenbach, K. R., Huang, Y., Zhang, R. J., Li, Z. Q., Cao, J. J., Baltensperger, U., El-Haddad, I.,
412 and Prevot, A. S. H.: New insights into PM_{2.5} chemical composition and sources in two major
413 cities in China during extreme haze events using aerosol mass spectrometry, *Atmospheric
414 Chemistry and Physics*, 16, 3207-3225, 10.5194/acp-16-3207-2016, 2016.

415 Feng, J. L., Hu, J. C., Xu, B. H., Hu, X. L., Sun, P., Han, W. L., Gu, Z. P., Yu, X. M., and Wu, M. H.:
416 Characteristics and seasonal variation of organic matter in PM_{2.5} at a regional background site
417 of the Yangtze River Delta region, China, *Atmospheric Environment*, 123, 288-297,
418 10.1016/j.atmosenv.2015.08.019, 2015.

419 Highwood, E. J., and Kinnersley, R. P.: When smoke gets in our eyes: the multiple impacts of
420 atmospheric black carbon on climate, air quality and health, *Environment international*, 32,
421 560-566, 10.1016/j.envint.2005.12.003, 2006.

422 Hu, J., Wang, Y., Ying, Q., and Zhang, H.: Spatial and temporal variability of PM_{2.5} and PM₁₀
423 over the North China Plain and the Yangtze River Delta, China, *Atmospheric Environment*, 95,
424 598-609, <http://dx.doi.org/10.1016/j.atmosenv.2014.07.019>, 2014.

425 Huang, R. J., Zhang, Y. L., Bozzetti, C., Ho, K. F., Cao, J. J., Han, Y. M., Daellenbach, K. R., Slowik, J.
426 G., Platt, S. M., Canonaco, F., Zotter, P., Wolf, R., Pieber, S. M., Bruns, E. A., Crippa, M., Ciarelli, G.,
427 Piazzalunga, A., Schwikowski, M., Abbaszade, G., Schnelle-Kreis, J., Zimmermann, R., An, Z. S.,
428 Szidat, S., Baltensperger, U., El Haddad, I., and Prevot, A. S. H.: High secondary aerosol
429 contribution to particulate pollution during haze events in China, *Nature*, 514, 218-222,
430 10.1038/nature13774, 2014.

431 Khan, M. F., Shirasuna, Y., Hirano, K., and Masunaga, S.: Characterization of PM_{2.5}, PM_{2.5-10}
432 and PM_{>10} in ambient air, Yokohama, Japan, *Atmospheric Research*, 96, 159-172,
433 <http://dx.doi.org/10.1016/j.atmosres.2009.12.009>, 2010.

434 Kim, H.-S., Huh, J.-B., Hopke, P. K., Holsen, T. M., and Yi, S.-M.: Characteristics of the major
435 chemical constituents of PM_{2.5} and smog events in Seoul, Korea in 2003 and 2004,
436 *Atmospheric Environment*, 41, 6762-6770, <http://dx.doi.org/10.1016/j.atmosenv.2007.04.060>,
437 2007.

438 Ling, Z. H., Guo, H., Cheng, H. R., and Yu, Y. F.: Sources of ambient volatile organic compounds
439 and their contributions to photochemical ozone formation at a site in the Pearl River Delta,
440 southern China, *Environmental Pollution*, 159, 2310-2319,
441 <https://doi.org/10.1016/j.envpol.2011.05.001>, 2011.

442 Liu, D., Li, J., Zhang, Y., Xu, Y., Liu, X., Ding, P., Shen, C., Chen, Y., Tian, C., and Zhang, G.: The use
443 of levoglucosan and radiocarbon for source apportionment of PM_{2.5} carbonaceous aerosols

444 at a background site in East China, *Environmental Science & Technology*, 47, 10454-10461, 2013.

445 Liu, D., Li, J., Cheng, Z. N., Zhong, G. C., Zhu, S. Y., Ding, P., Shen, C. D., Tian, C. G., Chen, Y. J.,
446 Zhi, G. R., and Zhang, G.: Sources of non-fossil-fuel emissions in carbonaceous aerosols during
447 early winter in Chinese cities, *Atmospheric Chemistry and Physics*, 17, 11491-11502,
448 10.5194/acp-17-11491-2017, 2017a.

449 Liu, J., Li, J., Zhang, Y., Liu, D., Ding, P., Shen, C., Shen, K., He, Q., Ding, X., and Wang, X.: Source
450 Apportionment Using Radiocarbon and Organic Tracers for PM_{2.5} Carbonaceous Aerosols in
451 Guangzhou, South China: Contrasting Local- and Regional-Scale Haze Events, *Environmental
452 Science & Technology*, 48, 12002-12011, 2014.

453 Liu, J., Li, J., Liu, D., Ding, P., Shen, C., Mo, Y., Wang, X., Luo, C., Cheng, Z., Szidat, S., Zhang, Y.,
454 Chen, Y., and Zhang, G.: Source apportionment and dynamic changes of carbonaceous
455 aerosols during the haze bloom-decay process in China based on radiocarbon and organic
456 molecular tracers, *Atmos. Chem. Phys.*, 16, 2985-2996, 10.5194/acp-16-2985-2016, 2016.

457 Liu, J., Ding, P., Zong, Z., Li, J., Tian, C., Chen, W., Chang, M., Salazar, G., Shen, C., Cheng, Z.,
458 Chen, Y., Wang, X., Szidat, S., and Zhang, G.: Evidence of Rural and Suburban Sources of Urban
459 Haze Formation in China: A Case Study From the Pearl River Delta Region, *Journal of
460 Geophysical Research: Atmospheres*, 123, 4712-4726, doi:10.1029/2017JD027952, 2018.

461 Liu, J. W., Li, J., Ding, P., Zhang, Y. L., Liu, D., Shen, C. D., and Zhang, G.: Optimizing isolation
462 protocol of organic carbon and elemental carbon for C-14 analysis using fine particulate
463 samples, *Atmospheric Environment*, 154, 9-19, 10.1016/j.atmosenv.2017.01.027, 2017b.

464 Liu, P., Zhang, C., Xue, C., Mu, Y., Liu, J., Zhang, Y., Tian, D., Ye, C., Zhang, H., and Guan, J.: The
465 contribution of residential coal combustion to atmospheric PM_{2.5} in northern China during

466 winter, *Atmos. Chem. Phys.*, 17, 11503-11520, 10.5194/acp-17-11503-2017, 2017c.

467 Mauderly, J. L., and Chow, J. C.: Health Effects of Organic Aerosols, *Inhalation Toxicology*, 20,
468 257-288, 10.1080/08958370701866008, 2008.

469 Paraskevopoulou, D., Liakakou, E., Gerasopoulos, E., Theodosi, C., and Mihalopoulos, N.:
470 Long-term characterization of organic and elemental carbon in the PM_{2.5}
471 fraction: the case of Athens, Greece, *Atmos. Chem. Phys.*, 14, 13313-13325,
472 10.5194/acp-14-13313-2014, 2014.

473 Park, S.-S., Jeong, J.-U., and Cho, S.-Y.: Group separation of water-soluble organic carbon
474 fractions in ash samples from a coal combustion boiler, *Asian Journal of Atmospheric*
475 *Environment*, 6, 67-72, 2012.

476 Perrone, M. R., Piazzalunga, A., Prato, M., and Carofalo, I.: Composition of fine and coarse
477 particles in a coastal site of the central Mediterranean: Carbonaceous species contributions,
478 *Atmospheric Environment*, 45, 7470-7477, <http://dx.doi.org/10.1016/j.atmosenv.2011.04.030>,
479 2011.

480 Pöschl, U.: *Atmospheric Aerosols: Composition, Transformation, Climate and Health Effects*,
481 *Angewandte Chemie International Edition*, 44, 7520-7540, 10.1002/anie.200501122, 2005.

482 Pratsinis, S., Ellis, E. C., Novakov, T., and Friedlander, S. K.: The Carbon Containing Component
483 of the Los Angeles Aerosol: Source Apportionment and Contributions to the Visibility Budget,
484 *Journal of the Air Pollution Control Association*, 34, 643-650, 10.1080/00022470.1984.10465792,
485 1984.

486 Schauer, J. J., Kleeman, M. J., Cass, G. R., and Simoneit, B. R. T.: Measurement of Emissions from
487 Air Pollution Sources. 2. C1 through C30 Organic Compounds from Medium Duty Diesel Trucks,

488 Environmental Science & Technology, 33, 1578-1587, doi:10.1021/es980081n, 1999.

489 Schauer, J. J., Kleeman, M. J., Cass, G. R., and Simoneit, B. R. T.: Measurement of Emissions from
490 Air Pollution Sources. 3. C₁-C₂₉ Organic Compounds from Fireplace Combustion of Wood,
491 Environmental Science & Technology, 35, 1716-1728, doi:10.1021/es001331e, 2001.

492 Schauer, J. J., Kleeman, M. J., Cass, G. R., and Simoneit, B. R. T.: Measurement of Emissions from
493 Air Pollution Sources. 5. C₁-C₃₂ Organic Compounds from Gasoline-Powered Motor Vehicles,
494 Environmental Science & Technology, 36, 1169-1180, doi:10.1021/es0108077, 2002.

495 Szidat, S., Ruff, M., Perron, N., Wacker, L., Synal, H.-A., Hallquist, M., Shannigrahi, A. S., Yttri, K.,
496 Dye, C., and Simpson, D.: Fossil and non-fossil sources of organic carbon (OC) and elemental
497 carbon (EC) in Göteborg, Sweden, Atmospheric Chemistry and Physics, 9, 1521-1535,
498 10.5194/acp-9-1521-2009, 2009.

499 Szidat, S., Salazar, G. A., Vogel, E., Battaglia, M., Wacker, L., Synal, H.-A., and Türler, A.: ¹⁴C
500 Analysis and Sample Preparation at the New Bern Laboratory for the Analysis of Radiocarbon
501 with AMS (LARA), Radiocarbon, 56, 561-566, 2014.

502 Weber, R. J., Sullivan, A. P., Peltier, R. E., Russell, A., Yan, B., Zheng, M., De Gouw, J., Warneke, C.,
503 Brock, C., Holloway, J. S., Atlas, E. L., and Edgerton, E.: A study of secondary organic aerosol
504 formation in the anthropogenic-influenced southeastern United States, Journal of Geophysical
505 Research: Atmospheres, 112, 2007.

506 Wei, N. N., Wang, G. H., Zhouga, D. Q., Deng, K., Feng, J. L., Zhang, Y. H., Xiao, D. T., and Liu, W.:
507 Source apportionment of carbonaceous particulate matter during haze days in Shanghai based
508 on the radiocarbon, J. Radioanal. Nucl. Chem., 313, 145-153, 10.1007/s10967-017-5267-1, 2017.

509 Zhang, Y.-L., Kawamura, K., Agrios, K., Lee, M., Salazar, G., and Szidat, S.: Fossil and Nonfossil

510 Sources of Organic and Elemental Carbon Aerosols in the Outflow from Northeast China,
511 Environmental Science & Technology, 50, 6284-6292, 10.1021/acs.est.6b00351, 2016.

512 Zhang, Y. L., Perron, N., Ciobanu, V. G., Zotter, P., Minguillón, M. C., Wacker, L., Prévôt, A. S. H.,
513 Baltensperger, U., and Szidat, S.: On the isolation of OC and EC and the optimal strategy of
514 radiocarbon-based source apportionment of carbonaceous aerosols, Atmospheric Chemistry
515 and Physics, 12, 10841-10856, 2012.

516 Zhang, Y. L., Huang, R. J., El Haddad, I., Ho, K. F., Cao, J. J., Han, Y., Zotter, P., Bozzetti, C.,
517 Daellenbach, K. R., Canonaco, F., Slowik, J. G., Salazar, G., Schwikowski, M., Schnelle-Kreis, J.,
518 Abbaszade, G., Zimmermann, R., Baltensperger, U., Prévôt, A. S. H., and Szidat, S.: Fossil vs.
519 non-fossil sources of fine carbonaceous aerosols in four Chinese cities during the extreme
520 winter haze episode of 2013, Atmospheric Chemistry and Physics, 15, 1299-1312,
521 10.5194/acp-15-1299-2015, 2015a.

522 Zhang, Y. L., Schnelle-Kreis, J., Abbaszade, G., Zimmermann, R., Zotter, P., Shen, R. R., Schafer,
523 K., Shao, L., Prevot, A. S., and Szidat, S.: Source Apportionment of Elemental Carbon in Beijing,
524 China: Insights from Radiocarbon and Organic Marker Measurements, Environ Sci Technol, 49,
525 8408-8415, 10.1021/acs.est.5b01944, 2015b.

526 Zhang, Y. L., Ren, H., Sun, Y. L., Cao, F., Chang, Y. H., Liu, S. D., Lee, X. H., Agrios, K., Kawamura,
527 K., Liu, D., Ren, L. J., Du, W., Wang, Z. F., Prevot, A. S. H., Szida, S., and Fu, P. Q.: High
528 Contribution of Nonfossil Sources to Submicrometer Organic Aerosols in Beijing, China,
529 Environmental Science & Technology, 51, 7842-7852, 10.1021/acs.est.7b01517, 2017.

530 Zhang, Y. X., Shao, M., Zhang, Y. H., Zeng, L. M., He, L. Y., Zhu, B., Wei, Y. J., and Zhu, X. L.:
531 Source profiles of particulate organic matters emitted from cereal straw burnings, Journal of

532 Environmental Sciences, 19, 167-175, 2007.

533 Zhi, G. R., Chen, Y. J., Feng, Y. L., Xiong, S. C., Li, J., Zhang, G., Sheng, G. Y., and Fu, J.: Emission
534 characteristics of carbonaceous particles from various residential coal-stoves in China,
535 Environmental Science & Technology, 42, 3310-3315, 10.1021/es702247q, 2008.

536 Zong, Z., Wang, X., Tian, C., Chen, Y., Qu, L., Ji, L., Zhi, G., Li, J., and Zhang, G.: Source
537 apportionment of PM_{2.5} at a regional background site in North China using PMF linked with
538 radiocarbon analysis: insight into the contribution of biomass burning, Atmospheric Chemistry
539 & Physics, 16, 11249-11265, 2016.

540

541

542

543 Table 1. Concentrations ($\mu\text{g C}/\text{m}^3$) of different carbon species and their ratios

Site	PM2.5	WSOC	WIOC	EC	OC	TC	OC/EC	TC/PM2.5
Beijing								
24-Oct-13	89.1	5.23	5.28	2.23	10.5	12.7	4.71	0.14
27-Oct-13	326	43.8	26.9	18.2	70.7	89.0	3.88	0.27
8-Jan-14	97.0	3.61	2.60	1.12	6.21	7.33	5.56	0.08
15-Jan-14	518	98.3	48.9	19.7	147	167	7.49	0.32
13-Apr-14	326	11.4	12.2	5.92	23.6	29.5	3.98	0.09
17-Apr-14	176	14.1	6.28	5.39	20.4	25.7	3.78	0.15
24-Aug-14	96.0	4.40	3.60	1.77	8.00	9.77	4.52	0.10
26-Aug-14	103	3.71	3.48	2.20	7.19	9.39	3.28	0.09
Shanghai								
8-Nov-13	176	9.56	20.6	7.49	30.1	37.6	4.02	0.21
11-Nov-13	67.2	1.88	2.56	1.02	4.44	5.46	4.37	0.08
22-Dec-13	81.8	4.16	5.07	2.82	9.23	12.1	3.27	0.15
28-Dec-13	216	9.51	17.2	9.73	26.7	36.4	2.75	0.17
4-Apr-14	168	5.37	9.77	4.59	15.1	19.7	3.30	0.12
7-Apr-14	110	4.63	4.19	2.20	8.81	11.0	4.00	0.10
10-Jul-14	128	6.25	5.72	3.49	12.0	15.5	3.43	0.12
Guangzhou								
22-Oct-13	79.3	9.09	7.41	3.62	16.5	20.1	4.56	0.25
27-Oct-13	124	8.79	14.0	5.80	22.8	28.6	3.93	0.23
22-Dec-13	40.1	4.90	2.92	1.73	7.83	9.56	4.51	0.24
4-Jan-14	159	48.9	20.4	8.04	69.2	77.3	8.61	0.49
28-Mar-14	61.0	10.3	6.06	5.98	16.4	22.3	2.74	0.37
9-Apr-14	124	23.3	13.2	13.5	36.4	50.0	2.69	0.40
1-Jul-14	34.5	2.07	2.90	2.70	4.97	7.66	1.84	0.22
7-Jul-14	120	11.7	11.8	8.09	23.5	31.6	2.90	0.26

544

545

546

547 Table 2. Relative contribution of fossil fuel sources to different carbon fractions

Site/Time	WSOC	WIOC	EC	OC	TC
Beijing					
24-Oct-13	0.37	0.33	0.67	0.35	0.41
27-Oct-13	0.40	0.39	0.63	0.39	0.44
8-Jan-14	0.63	0.49	0.72	0.57	0.60
15-Jan-14	0.65	0.74	0.77	0.68	0.69
13-Apr-14	0.56	0.44	0.75	0.50	0.55
17-Apr-14	0.51	0.48	0.75	0.50	0.55
24-Aug-14	0.45	0.43	0.77	0.44	0.50
26-Aug-14	0.56	0.49	0.79	0.53	0.59
Shanghai					
8-Nov-13	0.23	0.40	0.67	0.35	0.41
11-Nov-13	0.37	0.36	0.75	0.37	0.44
22-Dec-13	0.45	0.54	0.72	0.50	0.55
28-Dec-13	0.44	0.50	0.68	0.48	0.53
4-Apr-14	0.44	0.53	0.71	0.50	0.55
7-Apr-14	0.38	0.48	0.70	0.43	0.48
10-Jul-14	0.69	0.67	0.84	0.68	0.71
Guangzhou					
22-Oct-13	0.35	0.44	0.67	0.39	0.44
27-Oct-13	0.47	0.36	0.70	0.40	0.46
22-Dec-13	0.35	0.44	0.61	0.38	0.42
4-Jan-14	0.29	0.28	0.52	0.28	0.31
28-Mar-14	0.52	0.57	0.84	0.54	0.62
9-Apr-14	0.57	0.59	0.88	0.58	0.66
1-Jul-14	0.54	0.53	0.86	0.54	0.65
7-Jul-14	0.49	0.50	0.86	0.50	0.59

548

549

550

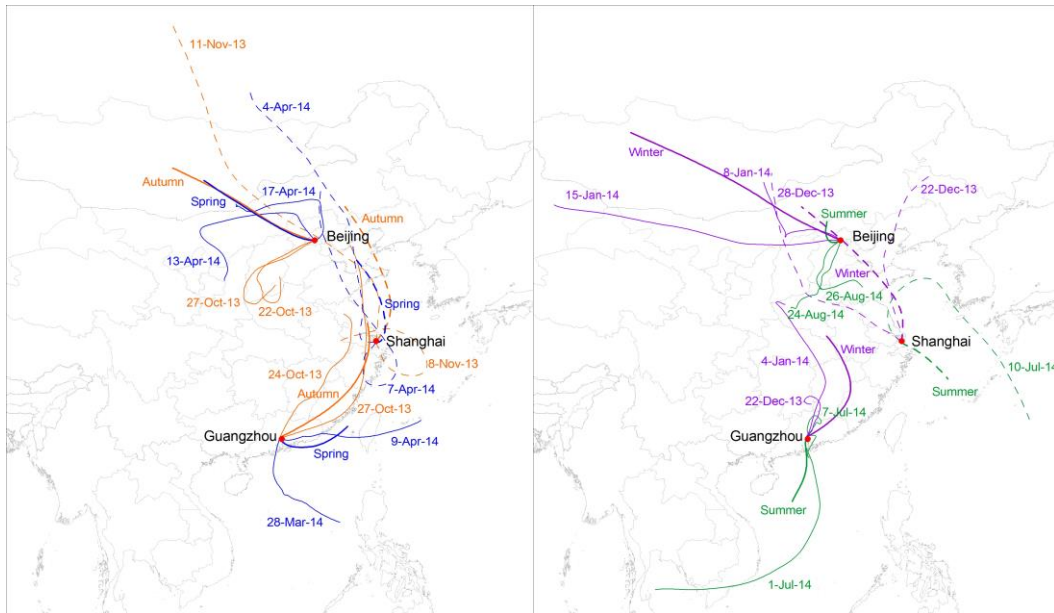
551 Table 3. Fossil fuel fraction of TC and EC in PM_{2.5} during 2012-2014 in three cities

Site/Time	Beijing		Shanghai		Guangzhou		Ref
	TC	EC	TC	EC	TC	EC	
Jan-2013(H)		74%		68%		68%	(Andersson et al., 2015)
Jan-13(L)	49%		43%		22%		(Huang et al., 2014)
Jan-13(H)	60%		46%		36%		
Jan-13(H)					53%	86%	(Liu et al., 2014)
Jan-13(H)					36%	66%	
Jan-13(L)					40%	66%	(Wei et al., 2017)
Jan-13 (H)				69%			
Mar- Apr, 2013(A)	44%	67%			54%	80%	(Liu et al., 2016)
Jul-13(H)					32%	76%	(Liu et al., 2018)
Jul-13(L)					60%	86%	
Oct-Nov-13(H)	37%	51%	33%	67%	29%	51%	(Liu et al., 2017a)
Oct-Nov-13(L)	30%	49%	29%	44%	41%	76%	

552 Note. H means higher PM_{2.5} concentration, L means lower PM_{2.5}, A means average

553 levels.

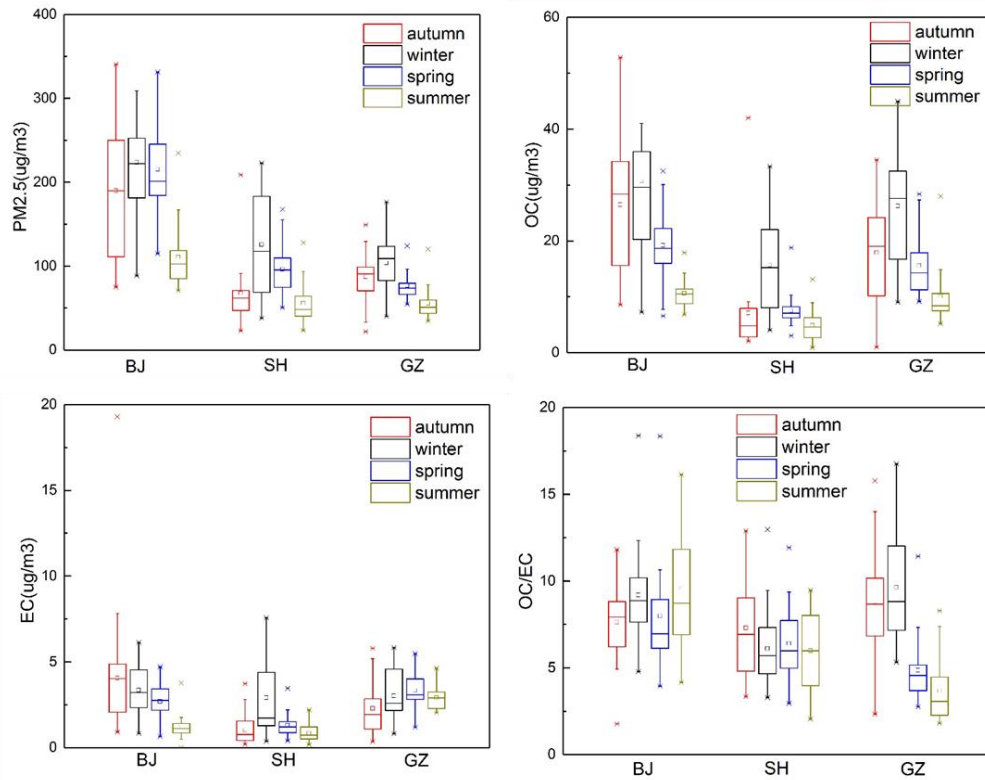
554



555

556 Figure 1. Air mass 3-day back trajectories at 6 h intervals for all samples are
 557 modeled at 500m above ground level by Air Resources Laboratory, National
 558 Oceanic and Atmospheric Administration
 559 (<http://ready.arl.noaa.gov/HYSPLIT.php>). Autumn, Winter, Spring and Summer
 560 mean the average 3-day back trajectories of all samples collected during each
 561 season.

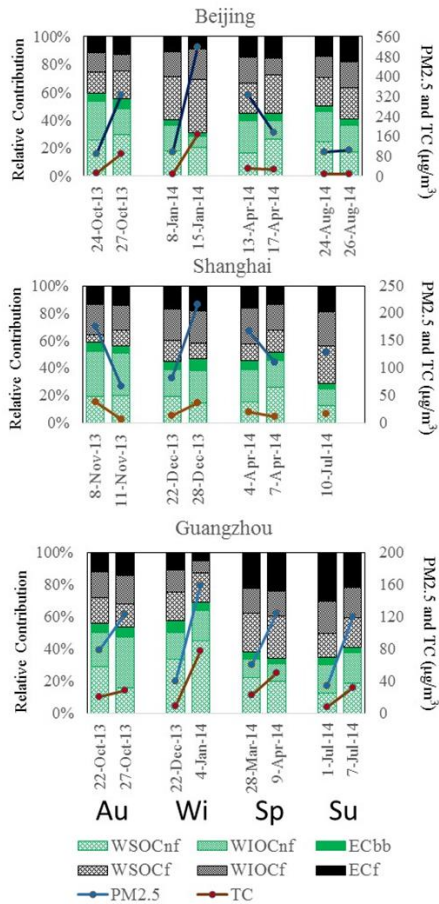
562



563

564 Figure 2. Box-and-whisker plots of mass concentrations of PM_{2.5}, OC, EC and
 565 EC/OC ratios in Beijing (BJ, total 110 samples), Shanghai (SH, total 110 samples)
 566 and Guangzhou (GZ, total 105 samples) during sampling periods 2013 -2014.
 567 The box represents the 25th (lower line), 50th (middle line) and 75th (top line)
 568 percentiles values, while the end of the lower and upper vertical line represents
 569 the 10th and 90th percentile values, respectively.

570

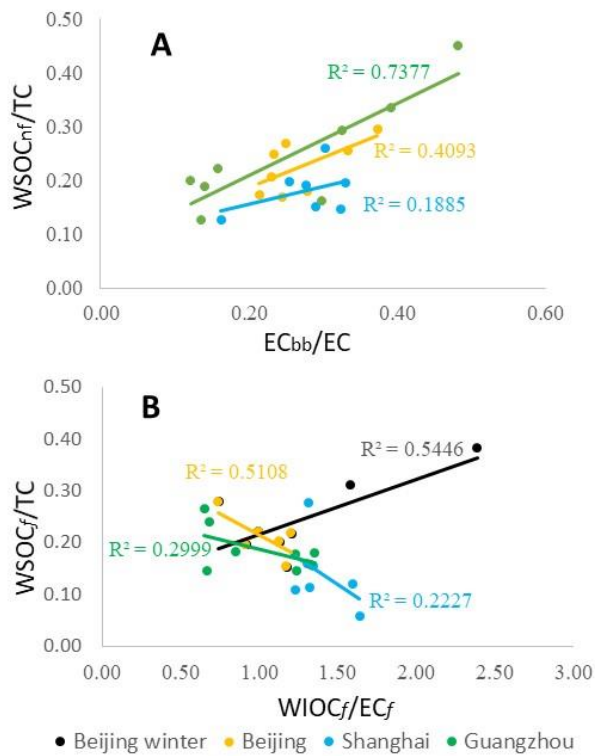


571

572 Fig. 3. The relative contributions of fossil EC (EC_i), fossil water-insoluble OC
 573 ($WIOC_i$), fossil water-soluble OC ($WSOC_f$), non-fossil EC (EC_{nf}), non-fossil
 574 water-insoluble OC ($WIOC_{nf}$), and non-fossil water-soluble OC ($WSOC_{nf}$) to total
 575 carbon (TC) and the concentrations of PM_{2.5} and TC in four seasons (autumn/Au,
 576 winter/Wi, spring/Sp, summer/Su) in Beijing, Shanghai and Guangzhou.

577

578



579

580

581 Fig. 4. Correlations of $WSOC_{nf}/TC$ vs. EC_{bb}/EC (A), and $WSOC_f/TC$ vs. $WIOC_f/EC_f$

582 (B). Beijing winter means all samples collected in Beijing; Beijing means winter

583 samples were excluded.

584

585